VLA MULTI-WAVELENGTH MICROWAVE OBSERVATIONS OF SATURN'S C AND B RINGS. Z. Zhang[1], A.G. Hayes[1], I. de Pater[4], D.E. Dunn[5], M.A. Janssen[2], P.D. Nicholson[1], J.N. Cuzzi[3], B.J. Butler[6], R.J. Sault[7], S. Chatterjee[1], [1]Astronomy Department, Cornell University, Ithaca, NY 14850, USA, [2]Jet Propulsion Laboratory, California Institute of Technology, Pasadena, CA, 91109, USA, [3]Space Science Division, Ames Research Center, NASA, Moffett Field, CA 94035, USA, [4]Astronomy Department, University of California, Berkeley, California 94720, USA, [5]Astronomy Department, Sierra College, Rocklin, CA 95677, USA, [6]National Radio Astronomy Observatory, P.O. Box O, Socorro, NM 87801, USA, [7]School of Physics, University of Melbourne, VIC 3010, Australia.

Introduction: We present multi-wavelength VLA observations in the microwave of Saturn's rings. The data were obtained over two observational windows and cover a range from the Q to S bands. We have placed the raw UV data through the pipeline calibration, bad data flagging, self-calibration, Fourier transformation and image de-convolution. The final calibrated observation maps contain information about the brightness temperature distribution in the Saturn disk and the ring system as seen from Earth (see Figure 1 as an example).

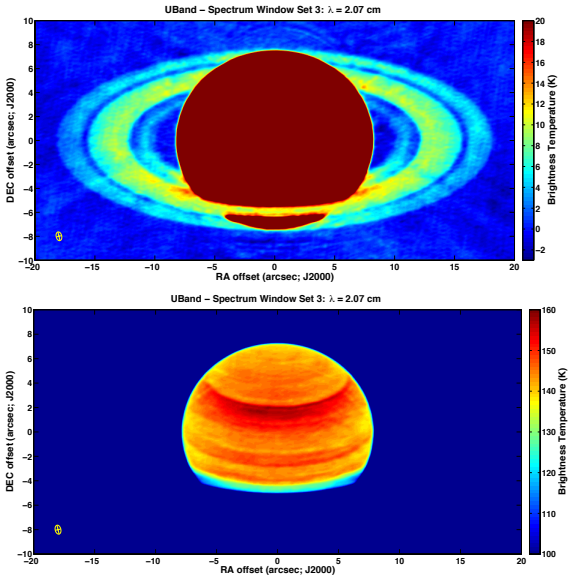

Figure 1. Final maps after calibration at U band as an example. The color range for the upper panel is set from -2 K to 20 K to show the structure of the rings. The color range on the lower panel is set from 100K to 160K to show the latitudinal variation of Saturn's thermal radiation. The yellow ellipses on the lower left of each panel indicate the synthesized beam sizes and corresponding position angles.

At the same time, we generated a synthetic image of Saturn and its rings using our Monte Carlo code and convolved it with the observational beam. We compared the final convolved simulated maps with the calibrated maps to investigate the ring particles' properties to be directly compared with those previously derived from the Cassini radiometry observations [1-2]. Key ring particle properties are determined in the C and B rings such as particle porosity and non-icy material fraction.

Results from Cassini Passive Radiometry observations at 2.2cm: [1] suggested a high porosity of 70%-75% for the C ring particles based on exceptionally high brightness observed at near-zero azimuthal angles. Furthermore, their results show that most regions in the C ring contain about 1-2% silicates, with an enhanced abundance of non-icy material concentrated in the middle C ring. When assumed to be mixed volumetrically ("intramixed") with water ice, this enhanced contamination reaches a maximum concentration of 6%-11% silicates by volume around a ring radius of 83,000 km (see Figure 2). As opposed to an intramixing model, they also consider a silicate-core, icy-mantle model to address the fact that silicates may be present in chunks instead of fine powder in the ring particles. Such a model naturally helps to account for the observed opacity distribution. They further proposed that the C ring has been continuously polluted by meteoroid bombardment since it first formed ~ 15 - 90 Myrs ago, while the middle C ring was further contaminated by an incoming Centaur, a rocky object torn apart by tides and ultimately broken into pieces that currently reside in the middle C ring.

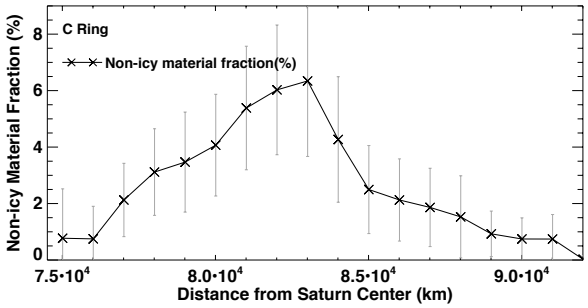

Figure 2. Radially varying non-icy material fraction derived from Cassini radiometry observation assuming 75% porosity in the "intramixed" model [1].

In a follow up paper, [2] expanded their analysis of the Cassini radiometer data to the B rings and derived

the non-icy material fraction in the B ring. Owing to the B ring's high opacity (*i.e.* high optical depth but low surface density), the best model fits suggest that the particles there are likely to be very porous, having values as high as 85% - 90%, with corresponding non-icy volume fractions of ~ 0.3% - 0.5% in the inner and outer B ring, and ~0.1% - 0.2% in the middle regions.

Results from VLA multi-wavelength observations: We find that the VLA observations in the U band of the C ring justify the results we obtained from the Cassini passive radiometer. We confirm that the C ring particles are seen to be highly porous and are characterized by a radially varying non-icy material fraction with an anomalously high fraction (hump) in the middle C ring (see Figure 2) when assuming that the non-icy material is intramixed within the ring particles. The application of the derived non-icy material fractions in the U band to K and Q band predict an intrinsic thermal emission that is higher than observed, which requires that the imaginary part of the non-icy material dielectric constant decrease with higher frequency. On the other hand, we find that the core-mantle model, which we proposed in [1] to account for the possibility that the bulk of the non-icy material (silicates) are present in large chunks embedded within the ring particles, naturally fits the observations at both low and high frequencies. If the former is the case, we should also observe similar results in the B ring. However, the non-icy material fraction in the B ring derived independently from the X, U, K and Q bands are very similar to each other, especially the X, U and K band data, when assuming 80% or 90% porosity, despite the different resolutions (see Figure 3). It either indicates that the non-icy material at middle C ring has different origin source than those in the B ring which was brought in through meteoroid flux or that the core-mantle model is the more likely case in agreement with the findings in [1], which naturally explains the lower than expected intrinsic thermal emission at higher frequencies. While deriving the best-fit non-icy material fraction in the B ring, we also notice that when assuming 55% porosity in B ring particles, the simulation cannot match the observation at Q band. The thermal emission contribution from pure water ice is already higher than the observed total amount of thermal emission at Q band. We also notice excessive amount of thermal emission contrition from water ice at Q band in the 80% porosity case. Therefore, the B ring particles are more likely to be as porous as 90%, which is consistent with its high opacity that also suggests porosity higher than 85%.

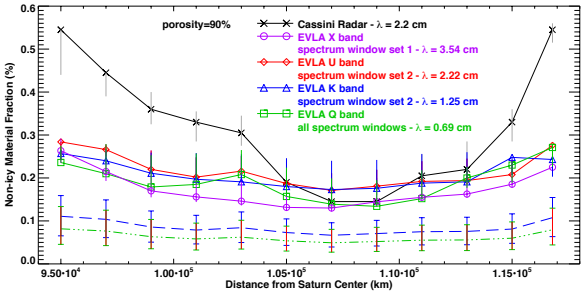

Figure 3. Non-icy material fraction in the B ring derived independently using the VLA observations in X (purple), U (red), K (blue) and Q (green) bands. The porosity is assumed to be 90%. The non-icy material dielectric constant has been assumed to remain constant in any of the wavelength band. The black curves show the results derived from Cassini passive radiometry observations. The blue (green) dashed line shows the expected non-icy material fraction in K (Q) band, if the imaginary part of the non-icy material dielectric constant shows same decreasing trend as found in the C ring intramixure model. The range of the expected non-icy material fraction profile for different phase function cases are indicated as the error bars.

In addition, because the VLA covers a more complete azimuthal angle range than the Cassini high-resolution radiometry observations, we are able to investigate the C ring brightness at azimuthal angles with absolute values ranging from 40 to 60 degrees. When we applied a pure Mie scattering phase function to all C ring particles, we found that the predicted scattering profile increases too steeply towards smaller angles in this range of azimuthal angles. This problem is resolved after we introduce a semi-empirical phase function for the large nonspherical particles. Assuming the intramixture model, we derived new non-icy material fractions and found that all of them show a similar non-icy material fraction trend. We further derived the corresponding core mantle model involving semi-empirical phase function. After introducing the semi-empirical phase function for large particles and the newly updated core mantle model, we are able to both fit the scattering profile well, and are able to match the U and K band data without assuming that the dielectric constant of the non-icy material is wavelength dependent in the microwave.

This work was supported by NASA SSW Program (Grant Number NNX15AJ95G).

References: [1] Z. Zhang et al (2017a) *Icarus, 281,* 297–321. [2] Z. Zhang. et al. (2017b) *submitted to Icarus*.